

Certainty of Stroke Diagnosis: Incremental Benefit with CT Perfusion over Noncontrast CT and CT Angiography¹

Julia Hopyan, BSc, MBBS
Anthony Ciarallo
Dar Dowlatshahi, PhD, MD
Peter Howard, MD
Verity John, MD
Robert Yeung, MD
Liyang Zhang, PhD
Jisung Kim
Genevieve MacFarlane, BSc
Ting-Yim Lee, PhD
Richard I. Aviv, MD, MRCP, FRCR

Purpose:

To systematically evaluate the diagnostic benefits and inter- and intraobserver reliability of an incremental computed tomographic (CT) protocol in the confirmation of clinically suspected stroke, with combined imaging and clinical data as the reference standard.

Materials and Methods:

Institutional review board approval was obtained, and participants gave informed consent. A total of 191 patients (mean age, 67 years \pm 16 [standard deviation]; 105 men) with stroke-like symptoms of no more than 3 hours duration were recruited. Blinded review was performed by four readers with limited stroke imaging experience. Diagnostic confidence was recorded on a five-point scale. Logistic regression analysis was used to calculate the difference between the real and observed diagnoses, adjusting for confidence. Predictive effects of observed diagnostic performance and confidence score were quantified with the entropy r^2 value. Sensitivity, specificity, and confidence intervals were calculated while accounting for multiple reader assessments. Receiver operating characteristic (ROC) analyses, including area under the ROC curve, were conducted for three modalities in combination with confidence score. Inter- and intraobserver agreement was established with the Cohen κ statistic.

Results:

The final diagnosis was infarct in 64% of the patients, transient ischemic attack in 18%, and stroke mimic in 17%. Large-vessel occlusion occurred in 70% of the patients with an infarct. Sensitivity for stroke determination with noncontrast CT, CT angiography, and CT perfusion increased by 12.4% over that with noncontrast CT and CT angiography and by 18.2% over that with only noncontrast CT for a confidence level of 4 or higher. The incremental protocol was more likely to enable confirmation of clinical stroke diagnosis (odds ratio, 13.3) than was noncontrast CT and CT angiography (odds ratio, 6.4) or noncontrast CT alone (odds ratio, 3.3). The area under the ROC curve was 0.67 for the combination of noncontrast CT and confidence score, 0.72 for the combination of CT angiography and confidence score, and 0.81 for the combination of CT perfusion and confidence score. Inter- and intraobserver agreement increased with progressive sequence use.

Conclusion:

An incremental stroke protocol that includes CT perfusion increases diagnostic performance for stroke diagnosis and inter- and intraobserver agreement.

©RSNA, 2010

¹ From the Department of Diagnostic Imaging, Division of Neuroradiology, Room AG 31, Sunnybrook Health Sciences Centre, 2075 Bayview Ave, Toronto, ON, Canada M4N 3M5. Received June 7, 2009; revision requested July 28; revision received August 20; accepted September 21; final version accepted October 20. Address correspondence to R.A. (e-mail: Richard.aviv@sunnybrook.ca).

Nonenhanced computed tomography (CT) is recommended by the American Heart Association as the initial modality of choice for stroke investigation (1). Nonenhanced, or noncontrast, CT is the preferred modality because of its accessibility, speed, and patient tolerance, thereby permitting the rapid triage of patients suspected of having experienced a stroke. Several studies have shown an association between baseline infarct size, final infarct volume, clinical outcome, and hemorrhagic transformation risk (2,3). If an infarct cannot be confirmed at baseline, then estimations of infarct size or tissue at risk cannot be made. This information remains one of the key lessons learned from the European Cooperative Acute Stroke Study II, where failure to recognize infarct in more than one-third of the middle cerebral artery territory contributed to hemorrhagic complications after administration of systemic lytic therapy (4).

While the absence of an identifiable infarct at imaging does not preclude stroke treatment in the appropriate clinical context, confirmation of infarct

presence provides visual reinforcement of clinical suspicion and allows a treatment decision to be made on the basis of the size and severity of ischemia (5,6). This is especially important as stroke mimics are reported in 10%–30% of all stroke presentations (7,8). We argue that infarct detection provides prognostic information for the attending clinician and facilitates appropriate stroke therapy. Detection of ischemia during a transient ischemic attack (TIA) similarly reinforces the clinical diagnosis and triggers the need for investigation into the underlying cardiovascular origin.

Proponents of magnetic resonance (MR) imaging–based acute strategies challenge whether CT has sufficient accuracy for use in infarction detection compared with the exquisite sensitivity of diffusion-weighted (DW) imaging (9–12). Early infarct detection with noncontrast CT remains a challenge. Sensitivity rates of 40%–60% have been described, and they depend on reviewer experience (6,13–16). The diagnostic performance of CT stroke protocols is improved with modification of window and level settings (17), interpretation of CT angiographic source images (18–21), and CT perfusion (22–31). Several studies report an association between occlusion site, recanalization rate, and clinical outcome (32–35). More recently, a vessel occlusion site was used as a surrogate marker of tissue at risk (36). These findings support the inclusion of CT angiography in current protocols.

The role of perfusion imaging in mismatch estimation remains controversial (18,24). Until perfusion mismatch ratio definitions are refined, many clinicians will consider perfusion

a research tool that contributes little to immediate acute stroke diagnosis and management. The additional contrast material requirement and radiation exposure serve as further deterrents to the use of CT perfusion. Information on the benefits of adding CT perfusion to existing noncontrast CT and combined noncontrast CT and CT angiography protocols in the confirmation of clinical stroke in consecutive patients who are suspected of having acute stroke and who are undergoing a modern acute CT protocol is sparse. In prior studies, researchers have reported on the performance of older generation scanners, recruited small numbers of nonconsecutive patients, and used expert readers and extended time windows (25,26,37–39). The purpose of this study was to systematically evaluate the diagnostic benefits and inter- and intraobserver reliability of an incremental CT protocol in the confirmation of clinically suspected stroke, with combined imaging and clinical data as the reference standard. We hypothesized that detection would be significantly improved with an incremental protocol.

Advances in Knowledge

- In a prospective and consecutive population presenting within 3 hours after onset of strokelike symptoms, CT perfusion images interpreted by relatively inexperienced readers significantly improve the performance for correct stroke diagnosis over that achieved with interpretation of noncontrast CT images alone or noncontrast CT images and CT angiographic source images.
- Among nonexpert readers, review of CT perfusion color maps increases correct stroke diagnosis four- and twofold over that achieved with review of noncontrast CT images alone and that achieved with review of noncontrast CT and CT angiographic source images, respectively; inter- and intraobserver agreement for correct stroke diagnosis is also significantly increased.

Implication for Patient Care

- CT perfusion as part of a comprehensive stroke protocol provides valuable additional information to relatively inexperienced readers for stroke detection over that provided by stroke protocols comprising only noncontrast CT images or noncontrast CT images and CT angiographic source images.

Materials and Methods

One author (T.Y.L.) is a consultant on CT perfusion software and has research

Published online

10.1148/radiol.09091021

Radiology 2010; 255:142–153

Abbreviations:

AIC = Akaike information criterion
 DW = diffusion weighted
 NIHSS = National Institutes of Health Stroke Scale
 ROC = receiver operating characteristic
 TIA = transient ischemic attack
 TPA = tissue plasminogen activator

Author contributions:

Guarantor of integrity of entire study, R.I.A.; study concepts/study design or data acquisition or data analysis/interpretation, all authors; manuscript drafting or manuscript revision for important intellectual content, all authors; manuscript final version approval, all authors; literature research, J.H., L.Z., T.Y.L., R.I.A.; clinical studies, A.C., D.D., P.H., V.J., R.I.A.; statistical analysis, L.Z., J.K., R.I.A.; and manuscript editing, J.H., P.H., V.J., R.Y., L.Z., J.K., G.M., T.Y.L., R.I.A.

See Materials and Methods for pertinent disclosures.

grant support from GE Healthcare (Waukesha, Wis). The other authors had control of data that might have presented a conflict of interest.

Study Design and Patient Cohort

All study procedures and medical chart review were approved by our institutional research ethics board. Signed consent was obtained from each patient or substitute decision maker for study enrollment, in accordance with the Health Care Consent act of 1996. Patients were prospectively recruited into a stroke database at a regional stroke center between January 2007 and June 2008. Database entry was performed by two research assistants (J.K., G.M.; 2 years of experience) and a neuroradiologist (R.I.A.; 5 years of experience) and was based on the following inclusion criteria: consecutive patients admitted under a code stroke designation to the emergency department within 3 hours after symptom onset; complete CT stroke protocol (noncontrast CT, CT angiography, and CT perfusion) performed at admission; and follow-up MR imaging (including a minimum of DW imaging and fluid-attenuated inversion recovery imaging) within 30 days after admission. A 30-day limit was established, as this represents an accepted time period for DW imaging findings to remain positive in patients who have experienced an acute stroke (40), although others have shown that abnormal signal intensity persists for up to 57 days after stroke (41). All patients examined with this protocol were included, irrespective of the final diagnosis and the presence or site of vessel occlusion. Patients who had a TIA and whose condition had not improved at the time of imaging were included; however, in accordance with the protocol, those whose condition was improving at the time of emergency department admission and patients with intracranial hemorrhage were not imaged with an acute stroke protocol and were thereby excluded from the cohort. Patients were also excluded if there were contraindications to iodinated contrast material injection (contrast material allergy, increased creatinine

level) or MR imaging (implant, metal exposure, mechanical valves, etc) and if MR imaging was performed outside of the 30-day cutoff. Clinical baseline data (age, sex, National Institutes of Health Stroke Scale [NIHSS] score, tissue plasminogen activator status and dose, cardiovascular risk factors, and time of tissue plasminogen activator administration and stroke onset) were obtained at the time of presentation to the emergency department. Of 361 patients who met the study entry criteria, 170 were excluded because of MR imaging contraindications ($n = 3$), because the interval between stroke onset and MR imaging was more than 30 days ($n = 130$), or because follow-up was not performed ($n = 37$). The reason why a large number of patients had delayed (>30 days after stroke) or absent MR imaging studies was a provincial policy of patient repatriation after acute stroke center care when local hospitals were initially bypassed.

CT Protocol

The CT stroke protocol was performed with a 64-section CT scanner (VCT; GE Healthcare) and included CT perfusion with 4-cm z plane coverage and CT angiography from the aortic arch to the vertex. Parameters were the same as those described previously (42). Follow-up MR imaging was performed in all included patients and comprised minimal DW imaging (repetition time msec/echo time msec, 8125/minimum; 26-cm field of view; 128×128 matrix; 5-mm section thickness; no intersection gap) and fluid-attenuated inversion recovery imaging (repetition time msec/echo time msec/inversion time msec, 8000/120/200; 22-cm field of view; 320×224 matrix; 5-mm section thickness; 1-mm intersection gap).

Image Processing

Commercially available software (CT Perfusion 3; GE Healthcare) was used to calculate parametric maps of cerebral blood flow, cerebral blood volume, and mean transit time by using baseline CT perfusion data, as described previously. Arterial input and venous output time-attenuation curves were gener-

ated, with regions of interest manually drawn by the CT technologist performing the study, usually in the anterior cerebral artery ipsilateral to the side of infarct and the superior sagittal sinus, respectively. All perfusion maps were generated by an experienced CT technician and, to reflect everyday practice, maps that were available on a picture archiving and communications system were those that were submitted for review. Postprocessing of CT angiographic source images was performed by CT technologists at the CT operator console. CT angiographic source image reformations were 4 mm thick with a 2-mm gap and were aligned to match the noncontrast CT image.

Review Protocol

Nonexpert reviewers were purposely selected for this study. There were two neurologists (V.J., D.D.; both with 1 year of clinical experience) who were in the midst of their stroke fellowship and two recently trained neuroradiologists (P.H., R.Y.; within 6 months of having completed their fellowship) who participated in this study. The review process was designed to simulate the usual order in which a stroke study is reviewed in our practice, beginning with interpretation of the noncontrast CT images and followed by interpretation of CT angiographic source images and CT perfusion color maps.

Prior to review, three anonymized Digital Imaging and Communications in Medicine folders were prepared and stored on a secure server. Each of the three folders contained 191 subfolders. The first folder contained only noncontrast CT images. The second folder contained noncontrast CT images and CT angiographic source images. The third folder contained noncontrast CT images, CT angiographic source images, and CT perfusion color maps. Individual studies were identified by a unique identifier. Only one folder was available to a reader at a time. Once a reader had completed a folder, the folder was removed and could not be accessed again.

Images were available for review with a Windows-based Digital Imaging

and Communications in Medicine viewer and a picture archiving and communication system (K-PACS, version 1.6.0; http://www.k-pacs.de/index.html?*session*id*key*=*session*id*val*). Reviewers were blinded to all clinical information, with the exception of the side of weakness. A custom database (Office Access 2003, SP3; Microsoft, Redmond, Wash) was produced, and all data were entered into it. One entry page was available for each patient and each assortment of noncontrast CT images alone, noncontrast CT images and CT angiographic source images, and noncontrast CT images, CT angiographic source images, and CT perfusion color maps. The database did not allow the reader to return to review previous decisions relating to the same patient or prior patients. Given the large number of cases per folder and the requirement to complete each folder from the first to last case, it took, on average, 1 month to complete a folder. For each patient, the reviewer was required to check whether imaging helped to confirm the clinical suspicion of stroke, side of infarct or ischemia, and/or hyperdense sign and to assign a five-point level of confidence score (1, stroke definitely absent; 2, stroke probably absent; 3, equivocal; 4, stroke probably present; 5, stroke definitely present). As previously described, the Alberta Stroke Program Early CT score was recorded for noncontrast CT images (43).

For CT perfusion color maps, an operational definition was used when any qualitative abnormality consistent with ischemia (cerebral blood flow or mean transit time deficit, no definite cerebral blood volume abnormality) or infarction (cerebral blood flow or mean transit time deficit with reduced cerebral blood volume) was seen. Prior to review, an expert reader (R.I.A., 5 years of experience) gave each reviewer a short tutorial that was based on three test cases and lasted approximately 10 minutes. The objectives of this brief tutorial were to ensure that each reviewer understood the purpose of the study, to briefly review the appearances of ischemia and infarction on images, and to familiarize the readers with the picture

archiving and communication system controls and database entry.

To assess intraobserver reliability, three reviewers reread 40 datasets chosen by selecting approximately every fifth case in the database. This repeat reading took place 1 month after the last prior data entry to avoid the unlikely event of recall bias. An experienced stroke neurologist (J.H., 3 years of experience) arbitrated the final diagnosis by reviewing the patient's clinical course and MR imaging findings with DW imaging within 30 days after presentation. For the purpose of this study, the most likely diagnosis was formulated by considering the combined clinical and radiologic features. A stroke was diagnosed if there was clinical or radiologic evidence of infarct or TIA; findings in these patients were considered true-positive, and these were the findings with which imaging observations were compared. A combined outcome measure is a logical and more accurate measure of outcome because if imaging alone were used, several misclassifications could arise, whereby patients with true clinical ischemia or infarction could be classified as having normal findings at follow-up imaging. These include patients who presented with symptoms of a TIA but in whom DW imaging findings were negative, those with symptomatic chronic carotid occlusion or stenosis, and those with poststroke thrombolysis in whom no DW imaging abnormality persists after iatrogenic or spontaneous recanalization. Other examples include patients with prior stroke and new clinical presentation in whom structural imaging or delayed DW imaging would be insufficient to enable us to determine the relevance of depicted lesions without prior comparative imaging. Early DW imaging would enable us to easily confirm an ischemic cause in these patients.

Statistical Analysis

Analyses were performed with a statistical software package (SAS, version 9.1; SAS Institute, Cary, NC). Results were expressed as either the mean \pm standard deviation or the median and interquartile range for quantitative variables and as proportions for categorical

findings. When the multireader measurements were not accounted for in the analysis, logistic regression analysis was used to predict real stroke diagnosis from the observed diagnosis of the incremental stroke protocol when adjusting for the corresponding confidence score. Odds ratios with 95% confidence intervals also were calculated. The real and observed diagnostic performance was recorded as 0 for absence and 1 for presence. The level of confidence score ranged from 1 to 5 in the model. The combined predictive effects of the observed diagnostic performance and the confidence score in the model were quantified with the entropy r^2 value (the higher the r^2 value, the better the model), which we calculated with the equation $r^2 = (L_O - L_M)/L_O$, where L_O and L_M represent the log likelihood (maximized-2) of the null model and the fitted model, respectively. Akaike information criterion (AIC) was calculated with the equation $AIC = L_M + 2 \cdot n$, where n is the number of parameters, and was also used to compare models among three modalities (the lower the AIC, the better the model). The diagnostic performance of the incremental protocols was also evaluated with receiver operating characteristic (ROC) curve analysis, without adjusting for multiple readers. For the optimum confidence score of 4 or greater, the area under the ROC curve was calculated for three modalities (noncontrast CT, CT angiography, and CT perfusion) in combination with confidence score.

To analyze the correlated data from four readers, generalized estimating equations were used to calculate the real stroke confirmation from observed diagnosis after adjusting for confidence score. For such correlated data, a generalized linear model with a binomial distribution (logit link function) was performed. The Genmod procedure can be used to fit models with the generalized estimating equation method. The quasilikelihood information criterion is a modification of the AIC to apply to models fit by generalized estimating equations. Smaller values of quasilikelihood information criterion indicate a better fitting model. Because of the

correlation resulting from multiple reader assessments on the same images and the various CT protocols applying to the same subject, the individual sensitivity ($\hat{S}e_i$) and specificity ($\hat{S}p_i$) were calculated from the cross table of real stroke diagnosis and observed diagnosis for each sequence. The overall sensitivity ($\hat{S}e$) was estimated with the equation $\hat{S}e = \frac{\sum_{i=1}^n N_i \hat{S}e_i}{\sum_{i=1}^n N_i}$, and its

variance, defined as $Var(\hat{S}e)$, was calculated with the equation $Var(\hat{S}e) = \frac{1}{n(n-1)} \sum_{i=1}^n \left[\left(\frac{N_i}{\bar{N}} \right)^2 (\hat{S}e_i - \hat{S}e)^2 \right]$. Thereafter, the 95% confidence interval was estimated. N_i indicates the total number of diagnoses considered for each patient and found positive at the time the real diagnosis was made, n indicates the total number of patients, and \bar{N} indicates $\sum N_i/n$. The estimate of specificity and its variance can be derived similarly, with $\hat{S}p_i$ and $\hat{S}p$ substituted into the previously mentioned equations (44). To compare sensitivity among three modalities, regression model of natural log of $\hat{S}e_i$ was performed to search for the association with modalities (1 for noncontrast CT, 2 for CT angiographic source images, and 3 for CT perfusion). The comparison of specificity was also conducted with the same method (45–47).

Inter- and intraobserver agreement were established with the Cohen κ statistic and considered moderate, substantial, and near perfect when the κ value was 0.41–0.60, 0.61–0.80, and 0.81–1.00, respectively. Results were considered significant at the 5% critical level ($P < .05$).

Results

Our study included 191 patients (105 men [55%]) with a mean age of 67 years \pm 16 (range, 18–95 years). The mean age of male patients (65 years \pm 16) was not significantly different ($P = .19$) from that of female patients (68 years \pm 15). Baseline demographic data—including symptomatic side, cardiovascular risk

factors, final clinical diagnosis, and size and site of vessel occlusion—are listed in Table 1. A hyperintense signal was present in 47 (38%) of 123 patients with a stroke. At presentation, median NIHSS and Alberta Stroke Program Early CT scores were 9 (interquartile range, 4–16) and 8 (interquartile range, 6–10), respectively. Median NIHSS score at presentation in patients with a TIA and those with stroke mimic was 4 (interquartile range, 2–9) and 5 (interquartile range, 2–8), respectively. The mean time from symptom onset to CT examination was 117 minutes \pm 59. Median MR imaging follow-up was 3 days (range, 0–29 days) in patients with an infarct and 3 days (range, 0–15 days) in patients with TIA and stroke mimic. A mean recombinant tissue plasminogen activator dose of 64 mg \pm 14 was administered in 52 (42%) of 123 patients with infarct. Table 2 shows the distribution of confidence scores for each sequence. Confidence scores of 4 or 5 were seen for 70% of noncontrast CT studies, 87% of noncontrast CT and CT angiographic studies, and 94% of noncontrast CT, CT angiographic, and CT perfusion studies.

Table 3 shows the progressive increase of multiple entropy r^2 values from 0.0491 to 0.224 and the decrease of AIC from 854.8 to 698.3 with the incremental protocol. The observed diagnosis was significantly related to the real diagnosis for all three protocols after adjusting for the confidence level ($P < .0001$). The noncontrast CT findings were 3.3 times more likely to help confirm stroke diagnosis (95% confidence interval: 2.26, 4.81); the noncontrast CT

Table 1

Baseline Demographic Data and Distribution of Abnormalities in the Study Cohort

Characteristic	No. of Patients
Male sex	105 (55)
Right side was symptomatic	91 (48)
Cardiovascular risk factors	
Hypertension	28 (15)
Diabetes mellitus	33 (17)
Coronary artery disease	18 (9)
Atrial fibrillation	37 (19)
Smoking	34 (18)
Hypercholesterolemia	15 (8)
History of stroke, TIA, or both	32 (17)
Final clinical diagnosis	
Stroke	123 (64)
Large vessel	86 (70)
ICA	24 (28)
ACA	2 (2)
M1 segment	30 (35)
M2 segment	12 (14)
M3 or M4 segment	11 (13)
PCA	3 (4)
Vertebrobasilar artery	2 (2)
PICA or SCA	2 (2)
Small vessel	37 (30)
TIA	36 (18)
Stroke mimic	32 (17)
Unknown	11 (34)
Conversion disorder, psychosis, or both	7 (22)
Complex migraine	6 (19)
Seizure	4 (12)
Sepsis	2 (6)
Parkinson disease	1 (3)
PRES	1 (3)

Note.—Data in parentheses are percentages. ACA = anterior cerebral artery, ICA = internal carotid artery, PCA = posterior cerebral artery, PICA = posterior inferior cerebellar artery, PRES = posterior reversible encephalopathy syndrome, SCA = superior cerebellar artery.

Table 2

Distribution of Confidence Scores for Each Sequence

Confidence Score	Noncontrast CT (n = 764)	Noncontrast CT and CT Angiography (n = 764)	Noncontrast CT, CT Angiography, and CT Perfusion (n = 764)
1	13 (1.7)	7 (0.9)	6 (0.8)
2	36 (4.7)	15 (2.0)	5 (0.7)
3	180 (23.6)	76 (10.0)	34 (4.4)
4	418 (54.7)	386 (50.5)	203 (26.6)
5	117 (15.3)	280 (36.6)	516 (67.5)

Note.—Data are numbers of studies. Data in parentheses are percentages.

Table 3

Progressive Increase of Multiple Entropy r^2 Value and Decrease of AIC with the Incremental Protocol

Sequence and Statistic	Logistic Regression Model			Generalized Estimating Equations Method		
	r^2 Value	AIC	P Value	Odds Ratio*	Quasiliikelihood Information Criterion	P Value
Noncontrast CT						
Model fit statistics	0.0491	854.8	ND	ND	863.0	ND
Observed diagnosis (yes or no)	ND	ND	<.0001	3.29 (2.26, 4.81)	ND	<.0001
Observed confidence score	ND	ND	.5651	0.94 (0.75, 1.17)	ND	.4773
Noncontrast CT and CT angiography						
Model fit statistics	0.117	794.4	ND	ND	804.0	ND
Observed diagnosis (yes or no)	ND	ND	<.0001	6.38 (4.13, 9.85)	ND	<.0001
Observed confidence score	ND	ND	.7796	1.04 (0.78, 1.40)	ND	.8191
Noncontrast CT, CT angiography, and CT perfusion						
Model fit statistics	0.224	698.3	ND	ND	709.6	ND
Observed diagnosis (yes or no)	ND	ND	<.0001	13.3 (8.57, 20.5)	ND	<.0001
Observed confidence score	ND	ND	.7796	1.04 (0.78, 1.40)	ND	.5346

Note.—Logistic regression analysis and generalized estimating equations were used to model the real stroke diagnosis on different observed diagnoses (only noncontrast CT; noncontrast CT and CT angiography; noncontrast CT, CT angiography, and CT perfusion) when adjusting for the corresponding confidence score. ND = no data.

* Data in parentheses are 95% confidence intervals.

and CT angiographic findings, 6.4 times more likely to help confirm stroke diagnosis (95% confidence interval: 4.13, 9.85); and the noncontrast CT, CT angiographic, and CT perfusion findings, 13.3 times more likely to help confirm stroke diagnosis (95% confidence interval: 8.57, 20.5). The combination of noncontrast CT, CT angiographic, and CT perfusion studies had a higher association with stroke confirmation than did the other studies.

We used ROC analysis to compare the ability to classify real versus observed diagnosis based on a prospectively defined reference standard and the individual reader response. A confidence level of 4 or greater was found to be the optimal cutoff point to achieve the highest sensitivity and specificity. For the optimum confidence score of 4 or greater, the area under the ROC curve increased progressively with more sequences, without adjusting for multiple readers. The area under the ROC curve was 0.67 for the combination of noncontrast CT and confidence score; 0.72 for the combination of noncontrast CT, CT angiography, and confidence score; and 0.81 for the combination of noncontrast CT, CT angiography, CT perfusion, and confidence score (Fig 1).

We used generalized estimating equations for correlation that resulted

Table 4

Diagnostic Performance for Stroke Detection with Incremental Study Review with ROC-determined Thresholds for Level of Confidence

Level of Confidence and Sequence	Sensitivity (%)	P Value	Specificity (%)	P Value
Confidence \geq 4				
Noncontrast CT	52.5 (44.9, 60.1)	1 vs 2: 0.244	84.4 (78.0, 90.8)	1 vs 2: 0.438
Noncontrast CT and CT angiography	58.3 (51.3, 65.2)	1 vs 3: 0.0003	85.0 (79.8, 90.3)	1 vs 3: 0.297
Noncontrast CT, CT angiography, and CT perfusion	70.7 (63.8, 77.6)	2 vs 3: 0.013	88.0 (80.9, 95.1)	2 vs 3: 0.788
Confidence \geq 3				
Noncontrast CT	49.2 (42.9, 55.6)	1 vs 2: 0.181	79.6 (73.6, 85.6)	1 vs 2: 0.246
Noncontrast CT and CT angiography	55.4 (49.0, 61.9)	1 vs 3: <0.0001	84.9 (79.8, 90.1)	1 vs 3: 0.303
Noncontrast CT, CT angiography, and CT perfusion	69.5 (62.7, 76.3)	2 vs 3: 0.006	85.7 (78.3, 93.0)	2 vs 3: 0.894

Note.—Data in parentheses are 95% confidence intervals. P values were calculated with the linear regression model of natural log (sensitivity) or log (specificity) and were dependant on the sequence (1 = noncontrast CT, 2 = noncontrast CT and CT angiography, 3 = noncontrast CT, CT angiography, and CT perfusion).

from multiple reader assessments. Table 3 shows there was a significant association between the real diagnosis and the observed diagnosis for all three protocols after adjusting for the confidence level ($P < .0001$). Noncontrast CT, CT angiography, and CT perfusion show a higher relationship with stroke confir-

mation (lower quasiliikelihood information criterion indicates the better fit). The combined diagnostic performance of the readers for ischemic or infarct detection is listed in Table 4. For the higher level of confidence (≥ 4), sensitivity increased from 5.8% to 12.4% for each additional sequence added. The

Figure 1

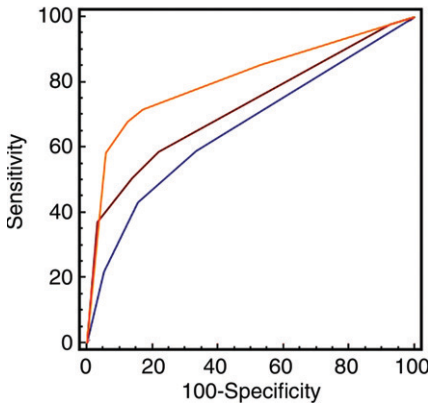


Figure 1: ROC curves show the diagnostic performance of the incremental stroke protocol in stroke detection, without adjusting for multiple readers. There is an increase in the area under the ROC curve with incremental sequence use. Blue = only noncontrast CT, brown = noncontrast CT and CT angiography, orange = noncontrast CT, CT angiography, and CT perfusion.

use of all three sequences increased sensitivity by 18.2% over that achieved with noncontrast CT alone. The sensitivity of noncontrast CT, CT angiography, and CT perfusion was significantly different compared with the sensitivity of noncontrast CT alone (70.7% vs 52.5%, $P = .0003$) and the sensitivity of noncontrast CT and CT angiography (70.7% vs 58.3%, $P = .013$). There was no significant difference between the sensitivity of noncontrast CT and the sensitivity of noncontrast CT and CT angiography ($P = .24$). Specificity remained unchanged as the number of sequences reviewed increased for this level of confidence (84.4% for noncontrast CT alone, 85.0% for noncontrast CT and CT angiography, and 88.0% for noncontrast CT, CT angiography, and CT perfusion; $P > .05$). A level of confidence of 3 or more increased the sensitivity of CT perfusion over that of CT angiography, but CT angiography and noncontrast CT demonstrated similar performances. Specificity increased by 6.2% and 14.1%, as more sequences were reviewed. Overall, CT perfusion increased specificity by 20.3% over that achieved with noncontrast CT alone. Overall, the percentage of uncertain responses with noncontrast CT, CT an-

Table 5

Cohen κ Determination of Interobserver Agreement for Four Readers

Reader No.	Noncontrast CT	Noncontrast CT and CT Angiography	Noncontrast CT, CT angiography, and CT Perfusion
1 vs 2	0.44	0.57	0.77
1 vs 3	0.28	0.34	0.78
1 vs 4	0.42	0.45	0.50
2 vs 3	0.30	0.47	0.69
2 vs 4	0.39	0.42	0.68
3 vs 4	0.28	0.44	0.70

Note.—Data are Cohen κ values.

Table 6

Cohen κ Determination of Intraobserver Agreement for Three Readers

Reader No.	Noncontrast CT	Noncontrast CT and CT Angiography	Noncontrast CT, CT Angiography, and CT Perfusion
1	0.40	0.46	0.77
2	0.60	0.77	0.88
3	0.52	0.31	0.65

Note.—Data are Cohen κ values and are based on a subset of 40 studies.

giography, and CT perfusion was 30%, 10%, and 6%, respectively.

Interobserver agreement was measured for each incremental protocol and increased from fair for noncontrast CT to moderate for CT angiography to substantial for CT perfusion (Table 5). Intraobserver agreement improved from moderate for noncontrast CT and CT angiography to substantial for CT perfusion (Table 6).

Discussion

The results of this study confirm our hypothesis that the addition of CT perfusion improves stroke diagnosis by relatively inexperienced readers over that achieved with noncontrast CT alone or a combination of noncontrast CT and CT angiography, with improved inter- and intraobserver agreement. The increased sensitivity is associated with stable or modestly improved specificity depending on the level of certainty, confirming that the improved performance was not due to overcalling. When interpretation of CT perfusion findings was more difficult, yielding an equivocal or higher level of confidence, no significant

change in performance was seen compared with reduced specificity for noncontrast CT and CT angiography. This study expands on the findings of earlier studies (25,26,37,38) by including a significantly larger study group with prospective data collection in consecutive patients presenting to an emergency department within 3 hours after the start of persistent strokelike symptoms. The final diagnosis was based on prospective evaluation of imaging and clinical parameters, with all patients undergoing MR imaging, including DW imaging, within 30 days of symptom onset. This definition allows accurate measurement of the performance of CT perfusion. Inter- and intraobserver agreement was high in a modest subset of patients. The study was designed to simulate the real-life environment by using clinically generated CT perfusion maps that were judged to be of appropriate image quality by experienced CT technicians, transferred to a picture archiving and communication system, and actually used when the examinations were originally performed. The choice to use reviewers with limited experience rather than expert reviewers was an

Figure 2

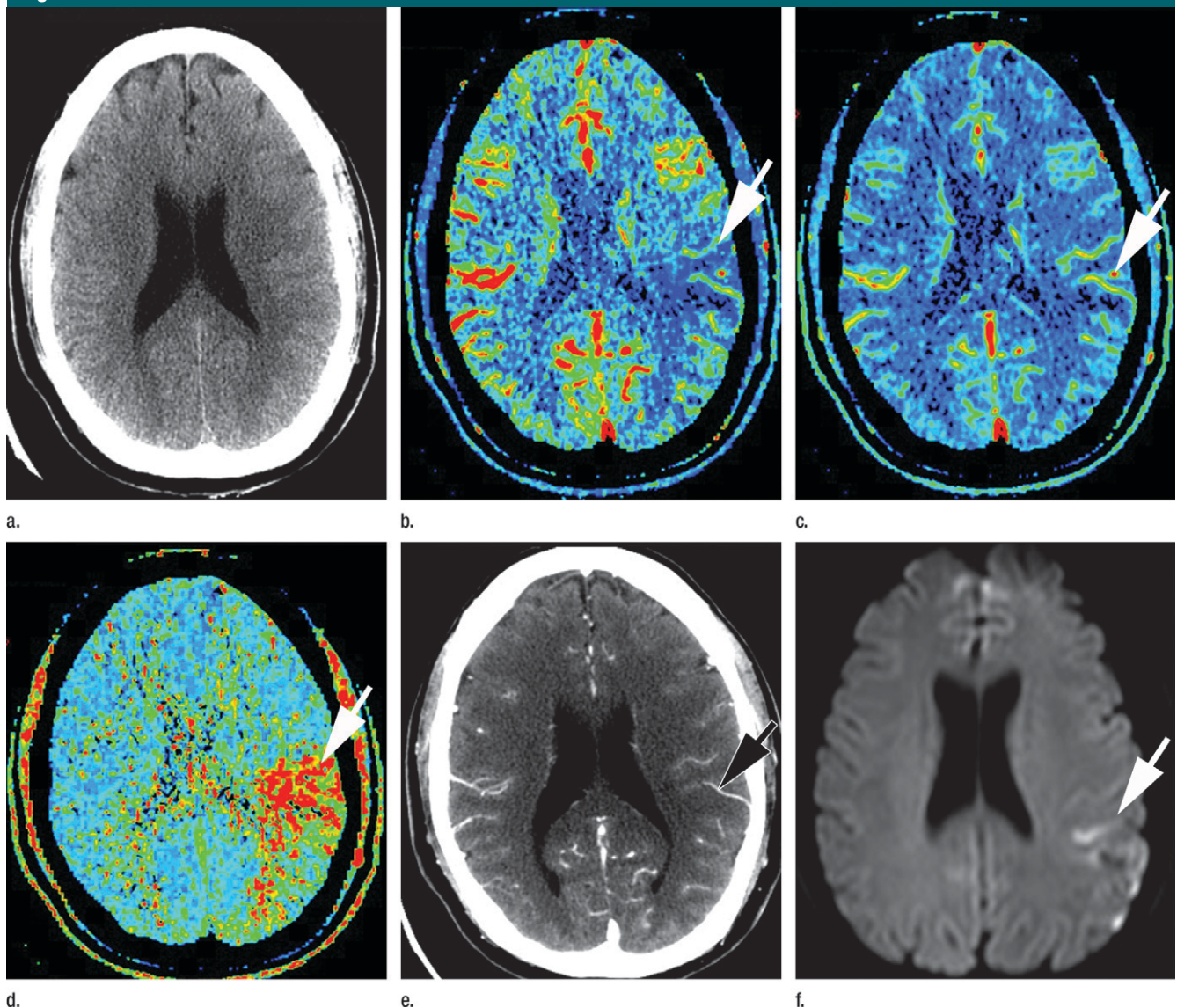


Figure 2: Images in a 42-year-old male patient who presented 70 minutes after symptom onset (NIHSS score, 10; 90-day modified Rankin scale score, 4). **(a)** Noncontrast CT image shows no abnormality. **(b)** Cerebral blood flow, **(c)** cerebral blood volume, and **(d)** mean transit time perfusion maps show a perfusion defect within the left parietal lobe (arrow). This lesion was most easily visible on **b** and **d**. **(e)** In retrospect, the hypoattenuation (arrow) was visible on the CT angiographic source image but was missed by all readers. No other parenchymal abnormality or vessel occlusion was seen. **(f)** Follow-up DW MR image helped confirm a focus of restriction (arrow), consistent with infarct.

acknowledgment of the fact that often the clinicians who review these studies are not stroke experts; instead, they have limited stroke experience. The use of an ROC analysis based on the level of confidence for stroke presence has been studied previously for CT angiography (20). This approach was shown to be more useful than an all-or-none

approach when milder levels of stroke are present.

We compared diagnostic performance and interobserver agreement with those in prior publications and confirmed similar performance for noncontrast CT (6,15–17). Higher detection rates with CT angiography usually are reported by expert readers within

an extended time period (20,46). Widening the interval from presentation to imaging improves infarct detection by allowing increased time for cytotoxic edema formation and visualization. Limited CT perfusion studies performed by expert readers have shown similar (37,38) or higher (25,26,39) performance for infarct detection. The

Figure 3

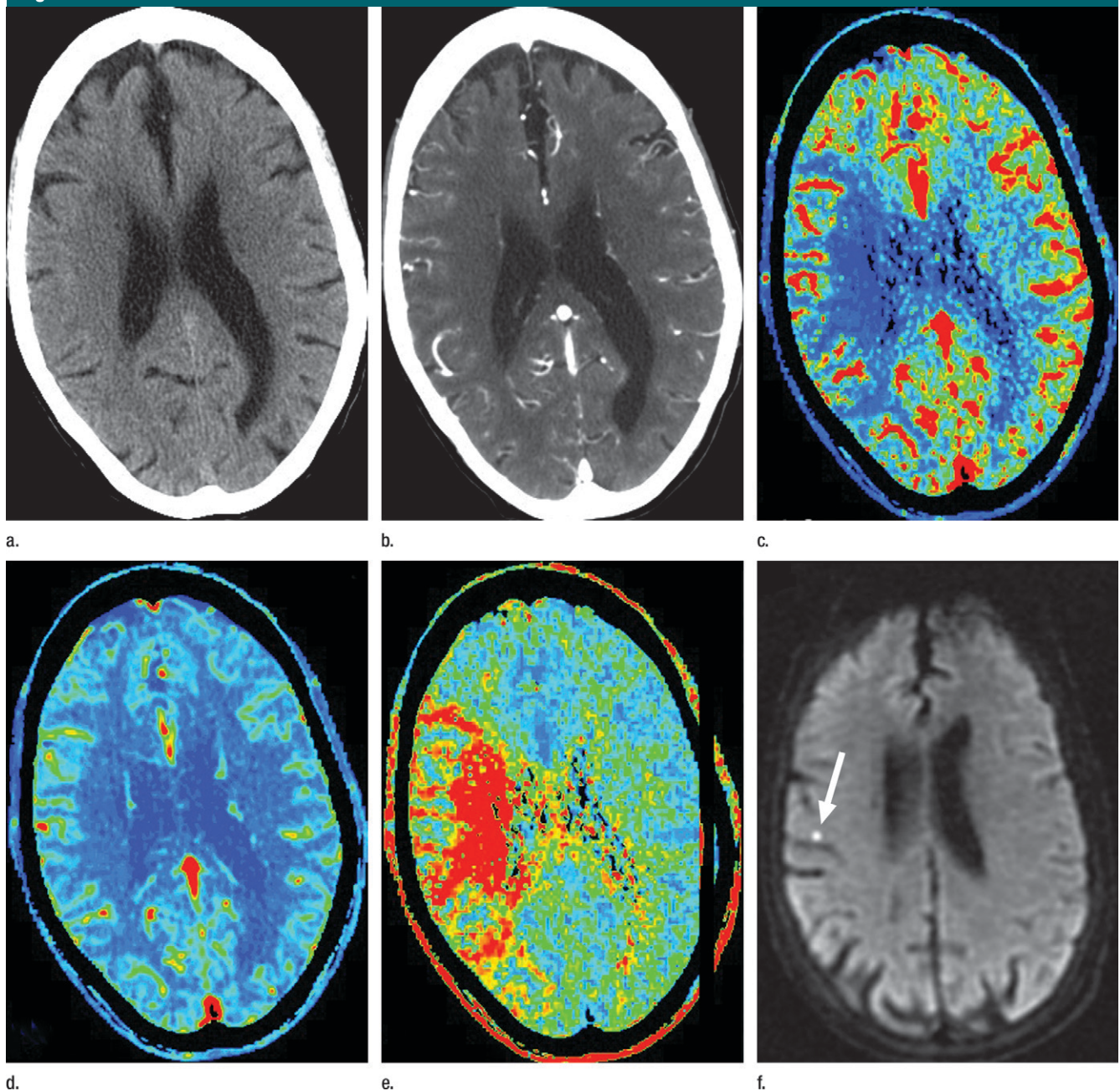


Figure 3: Images in a 77-year-old female patient who presented 59 minutes after onset of left hemiplegia due to right M1 occlusion (NIHSS score, 10). The patient received 48 mg of intravenous recombinant tissue plasminogen activator. (a) Noncontrast CT and (b) CT angiographic source images show no abnormality. (c) Cerebral blood flow, (d) cerebral blood volume, and (e) mean transit time perfusion maps show a large perfusion deficit with no definite infarcted tissue. (f) Follow-up DW MR image helped confirm a focus of restriction (arrow), consistent with infarct after successful recanalization.

modest median NIHSS and Alberta Stroke Program Early CT scores, inclusion of all patients suspected of having a stroke irrespective of vessel occlusion status and infarct location, reviewer ex-

perience, and inclusion of patients who presented with symptoms of TIA or stroke mimic contributed to a modestly lower performance compared with that of previous studies. Therefore, perfor-

mance reflects the number of small-profile lesions in the small-vessel group and the absence of visible baseline ischemia in patients with clinically diagnosed TIA. Despite these challenges,

our results demonstrate an incremental performance of an advanced stroke imaging protocol.

There is little argument that DW imaging provides a superior diagnostic performance for infarct detection than any CT-based protocol currently available; however limited resources, unique contraindications created by the MR imaging environment, and longer scan times argue in favor of the use of CT-driven protocols in the acute setting. The CT perfusion component of advanced stroke protocols adds 1–1.5 minutes of scanning time and 5–7 minutes of processing time until maps are available on a picture archiving and communication system when compared with noncontrast CT and CT angiographic protocols. This delay is comparable to the processing time required for CT angiographic multiplanar reformations. In addition to the potential but yet-to-be-realized benefits of penumbral imaging (32–35,42,47), an advanced CT protocol including CT perfusion is well adapted to the role of rapid triage of patients suspected of having had a stroke. The increased performance of CT perfusion in stroke detection is due to its ability to depict infarcts not readily visible on regular images because of the lack of a visible vessel occlusion or the presence of equivocal noncontrast CT and CT angiographic source images, parenchymal findings, or confounding remote large- or small-vessel infarcts and chronic microangiopathic change (Figs 2, 3). The detection of lesions is facilitated in these patients by the presence of a perfusion defect. Although limited parenchymal coverage remains a challenge, several techniques, including table toggle (48) and repeat CT perfusion at a higher level, have been reported (49). A greater number of detectors now allows for whole-head coverage; however, concerns about the radiation dose persist (50,51). The CT perfusion component of the current stroke protocol accounts for a radiation dose equivalent to that of noncontrast CT; therefore, we believe that the additional dose and the small radiation-induced risks are justified. Another limitation of CT perfusion is that chronic

proximal ICA occlusion is associated with prominent blood flow and transit time disturbances that are not necessarily indicative of acute ischemia or associated with stroke. Thus, these patients may be the cause of false-positive CT perfusion results in the unusual situation where the abnormal findings are contralateral to or considered incidental to stroke manifestation. Furthermore, when new hemodynamic or ischemic features arise, these are usually not discernable within the larger region of perfusion abnormality. Thus, cases with chronic occlusion should be interpreted with caution and should prompt DW imaging to exclude underlying infarct not discernable at CT perfusion.

In an attempt to simulate a real-world situation, CT images were reviewed incrementally, favoring the last study to be read. This was a purposeful design and facilitated a measure of incremental benefit for each additional sequence. The provision of side of lesion is known to favor noncontrast CT infarct detection and may have increased the sensitivity for diagnosis. Clinical data did not appear to improve the sensitivity of CT angiographic source images (20,21). Our use of less experienced readers may be construed as a potential limitation; however, this too was a purposeful design. CT perfusion is more widely available outside of tertiary referral hospitals, and in our experience, nonexpert readers are increasingly being required to interpret this data. Prior publications have shown the benefit of CT perfusion with expert readers; however, to our knowledge, no study has made use of less experienced readers in a prospective consecutive patient cohort. Another potential limitation was the inclusion of patients who underwent thrombolysis. As previously stated, a potentially successful recanalization without a DW imaging abnormality may result in misclassification as nonischemic if follow-up images alone are reviewed. A combined clinical and radiologic outcome measure prospectively arbitrated by a stroke neurologist facilitated correct final designation of each enrolled patient. In conclusion, an incremental stroke protocol includ-

ing CT perfusion increases diagnostic performance for stroke detection and inter- and intraobserver agreement.

Acknowledgments: We gratefully acknowledge our radiographic technicians, without whom this work would not have been possible.

References

1. Adams HP Jr, del Zoppo G, Alberts MJ, et al. Guidelines for the early management of adults with ischemic stroke: a guideline from the American Heart Association/American Stroke Association Stroke Council, Clinical Cardiology Council, Cardiovascular Radiology and Intervention Council, and the Atherosclerotic Peripheral Vascular Disease and Quality of Care Outcomes in Research Interdisciplinary Working Groups—the American Academy of Neurology affirms the value of this guideline as an educational tool for neurologists. *Stroke* 2007;38(5):1655–1711. [Published corrections appear in *Stroke* 2007;38(6):e38, *Stroke* 2007;38(9):e96.]
2. Singer OC, Humpich MC, Fiehler J, et al. Risk for symptomatic intracerebral hemorrhage after thrombolysis assessed by diffusion-weighted magnetic resonance imaging. *Ann Neurol* 2008;63(1):52–60.
3. Tanne D, Kasner SE, Demchuk AM, et al. Markers of increased risk of intracerebral hemorrhage after intravenous recombinant tissue plasminogen activator therapy for acute ischemic stroke in clinical practice: the Multicenter rt-PA Stroke Survey. *Circulation* 2002;105(14):1679–1685.
4. Hacke WK, Kaste M, Fieschi C, et al. Intravenous thrombolysis with recombinant tissue plasminogen activator for acute hemispheric stroke: the European Cooperative Acute Stroke Study (ECASS). *JAMA* 1995;274(13):1017–1025.
5. von Kummer R. Early major ischemic changes on computed tomography should preclude use of tissue plasminogen activator. *Stroke* 2003;34(3):820–821.
6. von Kummer R, Bourquain H, Bastianello S, et al. Early prediction of irreversible brain damage after ischemic stroke at CT. *Radiology* 2001;219(1):95–100.
7. Libman RB, Wirkowski E, Alvir J, Rao TH. Conditions that mimic stroke in the emergency department: implications for acute stroke trials. *Arch Neurol* 1995;52(11):1119–1122.
8. Kothari RU, Brott T, Broderick JP, Hamilton CA. Emergency physicians: accuracy in the diagnosis of stroke. *Stroke* 1995;26(12):2238–2241.

9. Fiebach JB, Schellinger PD, Jansen O, et al. CT and diffusion-weighted MR imaging in randomized order: diffusion-weighted imaging results in higher accuracy and lower interrater variability in the diagnosis of hyperacute ischemic stroke. *Stroke* 2002;33(9):2206–2210.
10. Lee LJ, Kidwell CS, Alger J, Starkman S, Saver JL. Impact on stroke subtype diagnosis of early diffusion-weighted magnetic resonance imaging and magnetic resonance angiography. *Stroke* 2000;31(5):1081–1089.
11. Lövblad KO, Baird AE, Schlaug G, et al. Ischemic lesion volumes in acute stroke by diffusion-weighted magnetic resonance imaging correlate with clinical outcome. *Ann Neurol* 1997;42(2):164–170.
12. Grotta JC, Chiu D, Lu M, et al. Agreement and variability in the interpretation of early CT changes in stroke patients qualifying for intravenous rTPA therapy. *Stroke* 1999;30(8):1528–1533.
13. Tomura N, Uemura K, Inugami A, Fujita H, Higano S, Shishido F. Early CT finding in cerebral infarction: obscuration of the lentiform nucleus. *Radiology* 1988;168(2):463–467.
14. Truwit CL, Barkovich AJ, Gean-Marton A, Hibri N, Norman D. Loss of the insular ribbon: another early CT sign of acute middle cerebral artery infarction. *Radiology* 1990;176(3):801–806.
15. Patel SC, Levine SR, Tilley BC, et al. Lack of clinical significance of early ischemic changes on computed tomography in acute stroke. *JAMA* 2001;286(22):2830–2838.
16. Wardlaw JM, Mielke O. Early signs of brain infarction at CT: observer reliability and outcome after thrombolytic treatment—systematic review. *Radiology* 2005;235(2):444–453.
17. Lev MH, Farkas J, Gemmete JJ, et al. Acute stroke: improved nonenhanced CT detection—benefits of soft-copy interpretation by using variable window width and center level settings. *Radiology* 1999;213(1):150–155.
18. Lev MH, Segal AZ, Farkas J, et al. Utility of perfusion-weighted CT imaging in acute middle cerebral artery stroke treated with intra-arterial thrombolysis: prediction of final infarct volume and clinical outcome. *Stroke* 2001;32(9):2021–2028.
19. Schramm P, Schellinger PD, Fiebach JB, et al. Comparison of CT and CT angiography source images with diffusion-weighted imaging in patients with acute stroke within 6 hours after onset. *Stroke* 2002;33(10):2426–2432.
20. Camargo EC, Furie KL, Singhal AB, et al. Acute brain infarct: detection and delineation with CT angiographic source images versus nonenhanced CT scans. *Radiology* 2007;244(2):541–548.
21. Aviv RI, Shelef I, Malam S, et al. Early stroke detection and extent: impact of experience and the role of computed tomography angiography source images. *Clin Radiol* 2007;62(5):447–452.
22. Wintermark M, Reichhart M, Cuisenaire O, et al. Comparison of admission perfusion computed tomography and qualitative diffusion- and perfusion-weighted magnetic resonance imaging in acute stroke patients. *Stroke* 2002;33(8):2025–2031.
23. Eastwood JD, Lev MH, Wintermark M, et al. Correlation of early dynamic CT perfusion imaging with whole-brain MR diffusion and perfusion imaging in acute hemispheric stroke. *AJNR Am J Neuroradiol* 2003;24(9):1869–1875.
24. Schramm P, Schellinger PD, Klotz E, et al. Comparison of perfusion computed tomography and computed tomography angiography source images with perfusion-weighted imaging and diffusion-weighted imaging in patients with acute stroke of less than 6 hours' duration. *Stroke* 2004;35(7):1652–1658.
25. Rai AT, Carpenter JS, Peykanu JA, Popovich T, Hobbs GR, Riggs JE. The role of CT perfusion imaging in acute stroke diagnosis: a large single-center experience. *J Emerg Med* 2008;35(3):287–292.
26. Wintermark M, Fischbein NJ, Smith WS, Ko NU, Quist M, Dillon WP. Accuracy of dynamic perfusion CT with deconvolution in detecting acute hemispheric stroke. *AJNR Am J Neuroradiol* 2005;26(1):104–112.
27. Popiela T, Pera J, Chrzan R, Wloch D, Urbanik A, Slowik A. Interobserver agreement in perfusion computed tomography evaluation in acute ischaemic stroke. *Neur Neurochir Pol* 2008;42(5):391–395.
28. Aviv RI, Mandelcorn J, Chakraborty S, et al. Alberta Stroke Program Early CT Scoring of CT perfusion in early stroke visualization and assessment. *AJNR Am J Neuroradiol* 2007;28(10):1975–1980.
29. Lin K, Rapalino O, Law M, Babb JS, Siller KA, Pramanik BK. Accuracy of the Alberta Stroke Program Early CT Score during the first 3 hours of middle cerebral artery stroke: comparison of noncontrast CT, CT angiography source images, and CT perfusion. *AJNR Am J Neuroradiol* 2008;29(5):931–936.
30. Tan JC, Dillon WP, Liu S, Adler F, Smith WS, Wintermark M. Systematic comparison of perfusion-CT and CT-angiography in acute stroke patients. *Ann Neurol* 2007;61(6):533–543.
31. Schaefer PW, Barak ER, Kamalian S, et al. Quantitative assessment of core/penumbra mismatch in acute stroke: CT and MR perfusion imaging are strongly correlated when sufficient brain volume is imaged. *Stroke* 2008;39(11):2986–2992.
32. Parsons MW, Barber PA, Chalk J, et al. Diffusion- and perfusion-weighted MRI response to thrombolysis in stroke. *Ann Neurol* 2002;51(1):28–37.
33. Albers GW, Thijs VN, Wechsler L, et al. Magnetic resonance imaging profiles predict clinical response to early reperfusion: the diffusion and perfusion imaging evaluation for understanding stroke evolution (DEFUSE) study. *Ann Neurol* 2006;60(5):508–517.
34. Hacke W, Albers G, Al-Rawi Y, et al. The Desmoteplase in Acute Ischemic Stroke Trial (DIAS): a phase II MRI-based 9-hour window acute stroke thrombolysis trial with intravenous desmoteplase. *Stroke* 2005;36(1):66–73.
35. Furlan AJ, Eyding D, Albers GW, et al. Dose Escalation of Desmoteplase for Acute Ischemic Stroke (DEDAS): evidence of safety and efficacy 3 to 9 hours after stroke onset. *Stroke* 2006;37(5):1227–1231.
36. Efficacy and safety study of desmoteplase to treat acute ischemic stroke (DIAS-3). *ClinicalTrials.gov* Web site. <http://clinicaltrials.gov/ct2/show/NCT00790920?term=NCT00790920&rank=00790921>. Updated October 5, 2009. Accessed May 15, 2009.
37. Kloska SP, Nabavi DG, Gaus C, et al. Acute stroke assessment with CT: do we need multimodal evaluation? *Radiology* 2004;233(1):79–86.
38. Scharf J, Brockmann MA, Daffertshofer M, et al. Improvement of sensitivity and interrater reliability to detect acute stroke by dynamic perfusion computed tomography and computed tomography angiography. *J Comput Assist Tomogr* 2006;30(1):105–110.
39. Röther J, Jonetz-Mentzel L, Fiala A, et al. Hemodynamic assessment of acute stroke using dynamic single-slice computed tomographic perfusion imaging. *Arch Neurol* 2000;57(8):1161–1166.
40. Lansberg MG, Thijs VN, O'Brien MW, et al. Evolution of apparent diffusion coefficient, diffusion-weighted, and T2-weighted signal intensity of acute stroke. *AJNR Am J Neuroradiol* 2001;22(4):637–644.
41. Eastwood JD, Engelter ST, MacFall JF, Delong DM, Provenzale JM. Quantitative

- assessment of the time course of infarct signal intensity on diffusion-weighted images. *AJNR Am J Neuroradiol* 2003;24(4):680-687.
42. Murphy BD, Fox AJ, Lee DH, et al. White matter thresholds for ischemic penumbra and infarct core in patients with acute stroke: CT perfusion study. *Radiology* 2008;247(3):818-825.
 43. Barber PA, Demchuk AM, Zhang J, Buchan AM. Validity and reliability of a quantitative computed tomography score in predicting outcome of hyperacute stroke before thrombolytic therapy: ASPECTS study group—Alberta Stroke Programme Early CT Score. *Lancet* 2000;355(9216):1670-1674.
 44. Zhou XH, Obuchowski NA, McClish DK. The sensitivity and specificity of clustered binary data. In: Balding DJ, Bloomfield P, Cressie NAC, eds. *Statistical methods in diagnostic medicine*. New York, NY: Wiley, 2002; 104-106.
 45. Pepe MS. Regression for true and false positive fractions. In: *The statistical evaluation of medical tests for classification and prediction*. New York, NY: Oxford University Press, 2003; 51-57.
 46. Coutts SB, Lev MH, Eliasziw M, et al. ASPECTS on CTA source images versus unenhanced CT: added value in predicting final infarct extent and clinical outcome. *Stroke* 2004;35(11):2472-2476.
 47. Murphy BD, Fox AJ, Lee DH, et al. Identification of penumbra and infarct in acute ischemic stroke using computed tomography perfusion-derived blood flow and blood volume measurements. *Stroke* 2006;37(7):1771-1777.
 48. Youn SW, Kim JH, Weon YC, Kim SH, Han MK, Bae HJ. Perfusion CT of the brain using 40-mm-wide detector and toggling table technique for initial imaging of acute stroke. *AJR Am J Roentgenol* 2008;191(3):W120-W126.
 49. Wintermark M, Smith WS, Ko NU, Quist M, Schnyder P, Dillon WP. Dynamic perfusion CT: optimizing the temporal resolution and contrast volume for calculation of perfusion CT parameters in stroke patients. *AJNR Am J Neuroradiol* 2004;25(5):720-729.
 50. Murayama K, Katada K, Nakane M, et al. Whole-brain perfusion CT performed with a prototype 256-detector row CT system: initial experience. *Radiology* 2009;250(1):202-211.
 51. Yang CY, Chen YF, Lee CW, et al. Multi-phase CT angiography versus single-phase CT angiography: comparison of image quality and radiation dose. *AJNR Am J Neuroradiol* 2008;29(7):1288-1295.